Moisture-Induced Alumina Scale Spallation: The Hydrogen Factor

James L. Smialek
NASA Glenn Research Center
Cleveland, OH 44135

Abstract

For some time our community has been concerned with interfacial spallation of protective alumina scales, not just upon immediate cooldown, but as a time-delayed phenomenon. Moisture-induced delayed spallation (MIDS) and desktop spallation (DTS) of TBC's refer to this process. It is most apparent for relatively adherent alumina scales that have survived cool down in a dry environment, built up considerable thickness and strain energy, and have been somewhat damaged, such as by cyclic oxidation cracking. Indeed, a "sweet zone" can be defined that maximizes the observed effect as a function of all the relevant factors. Moisture has been postulated to serve as a source of interfacial hydrogen embrittlement derived from reaction with aluminum in the alloy at an exposed interface. The purpose of this monograph is to trace the close analogy of this phenomenon to other hydrogen effects, such as embrittlement of aluminides and blistering of alloys and anodic alumina films. A formalized, top-down, logic tree structure is presented as a guide to this discussion. A theoretical basis for interfacial weakening by hydrogen is first cited, as are demonstrations of hydrogen as a reaction product or detected interfacial species. Further support is provided by critical experiments that produce the same moisture effect, but by isolating hydrogen from other potential causative factors. These experiments include tests in H_2-containing atmospheres or cathodic hydrogen charging.

Forward

There are numerous reported instances of moisture-induced spallation of alumina scales formed by high temperature oxidation. These occur under ambient conditions and are often discussed in terms of analogous phenomena for clarification and hypothetical mechanisms. Accordingly, it has been proposed that hydrogen, as a by-product of a room temperature moisture-alloy reaction, plays a key role in triggering spallation by affecting the interfacial scale-metal strength [**1,2**]. Such an effect is not at all unexpected considering ab initio models and interfacial toughness measurements that include hydrogen effects. Many similar attributes of hydrogen-related phenomena are sited as circumstantial evidence for this scale spallation mechanism, including hydrogen embrittlement of aluminides and blistering of anodic scales. The details of these supporting phenomena are not always fully presented. Furthermore, inductive arguments have generally been presented, as from the bottom up, citing scale spallation phenomenology, then generalizing to an overriding principal. It is the purpose of this monograph to present a deductive argument, restructured from the top down. We start with general principals, show parallels of several similar phenomena, and elaborate somewhat on the supporting evidence in each specific case. The intent is to present the proposed mechanism from a broader, more formalized perspective. Hopefully, this structured framework may point the way toward more revealing experiments and testing of the basic hypotheses.

The basic elements and guide are provided in the schematic entitled "The Hydrogen Factor: Logic Tree," **Figure 1**. The implied argument is that the MIDS and DTS phenomena follow

from a logical flow of basic reaction chemistry and interfacial bonding theory. The similarities and analogies to other related phenomena provide the hypothesis that one single mechanism applies across the board. The case is strengthened or in some cases proven by actual detection of interfacial hydrogen and elimination of all other factors except hydrogen. According to this scheme, we first try to justify (I) the generation of hydrogen from moisture in the presence of transition metals. Then (II) theoretical results for the detrimental effects of hydrogen on the strength of the alumina-metal bond are presented. A number of analogous phenomenological observations (III), believed to derive from these premises, are compared. Two factors of support are discussed for each of the phenomena: (IV) the detection of hydrogen at the weakened interface and (V) critical experiments isolating hydrogen effects from other possible ambient factors. This basic outline will be followed after presenting the attributes of both hydrogen embrittlement and moisture-induced spallation.

General Attributes of Hydrogen Embrittlement

Hydrogen embrittlement has been a widespread metallurgical issue for many decades. Accordingly, it has received an enormous amount of attention, from both the application and fundamental mechanism arenas. For the present purposes, it will suffice to highlight the most common attributes of the phenomenon, which can be found in any review or treatise on the subject.

Often an aqueous exposure is involved. This allows for global (e.g., galvanic) or local (pitting) electrochemical cells to produce a (-) cathodic driving force, attracting H^+ ions. As such, it is often enhanced by acidic conditions and sometimes found in cases of pickling, electropolishing, or electroplating. The maximum effect is usually observed near room temperature. This is where chemical activity and hydrogen mobility are high enough to produce and inject H into the material, but not so high as to promote its exit and loss by H_2 gas evolution. High pressure hydrogen gas or H_2S are other sources of a high hydrogen fugacity. Classic hydrogen embrittlement had first been associated with high strength ferritic (BCC) steels, but it has since been found in FCC stainless steels, Ni-base superalloys, and Al alloys, as well as a number of intermetallic compound phases.

A triaxial stress state favors the phenomenon. This provides a volumetric expansion, favorable sites attracting interstitial hydrogen, and diminished ability to blunt via plastic deformation. Triaxiality exists ahead of an exisiting crack tip and provides a zone of hydrogen accumulation. Once a crack nucleates and begins to grow, it often arrests until additional hydrogen can diffuse ahead of the crack tip and provide a new embrittled zone. Thus, discontinuous subcritical crack growth is a common attribute. Accordingly, the phenomenon becomes apparent only at certain strain rates, low enough to allow hydrogen diffusion, but fast enough to prevent complete loss by recombination and gaseous escape.

Since preferential, short circuit diffusion of hydrogen often applies, grain boundary fracture, though not necessary, is another frequent attribute. A negative synergy is often observed when other detrimental grain boundary segregants are present, such as S, P, or C. Furthermore, H-H recombination poisons in the environment, such as S and As, favor H injection (embrittlement) over escape as gaseous H_2.

The fundamental basis for hydrogen embrittlement is not fully resolved and remains an active topic of discussion. On one hand, ab initio studies have made a case for decreased M-M bond

strength for H-contaminated interfaces. On the other, a mechanism supporting, paradoxically, enhanced local *plasticity*, describes 'embrittlement' and interfacial weakening due to a thin network of highly mobile dislocations. For the present purpose of explaining moisture induced scale spallation, any hydrogen embrittlement mechanism allowing for decreased interfacial strength is acceptable. The details of various possible, but unproven, atomistic mechanisms are beyond the scope of this discussion.

Moisture-Induced Delayed Spallation (M.I.D.S.)

Proposed mechanism.
The elementary steps in the process are shown schematically in **Figure 2**. It can be postulated that local electrochemical cells develop at exposed oxide-metal interfaces in moist environments. Here H_2O is adsorbed on the exposed metal and dissociates to $(OH)^-$ and H^+. The amount of adsorption is a function of the relative humidity and has been discussed in regard to MIDS [**3**]. Anodic oxidation of aluminum from the alloy to Al^{+3} occurs at active exposed metal sites, resulting in $Al(OH)_3$ (or $Al_2O_3 \cdot nH_2O$). This frees e^- cathodically at protected (passivated) areas, attracting and reducing H^+. Hydrogen then diffuses interstitially under the scale. The biaxial tension, produced at the metal interface by CTE mismatch with the scale after cooling, provides an attraction for hydrogen.

Scale segments autocatalytically debond when the hydrogen concentration reaches a critical limit, reducing the interface toughness to where it can be overcome by the stored strain energy in the scale. This feature derives from the observation that scales directionally 'unzip' as humid air is allowed localized access to an exposed interface. It is also proposed that the scale cracking and spallation process itself is near instantaneous (τ_{spall3}), previously requiring some finite time for water dissociation and hydrogen diffusion ($\tau_{incubate2}$), relegating the remaining scale to much longer residence times ($\tau_{intact1}$), or indefinite immunity as stressed are relieved adjacent to the numerous spallation sites.

General phenomenological attributes. The early manifestations of this phenomenon were associated with a time factor after cooling from high temperature oxidation, i.e., after the sample was removed from a relatively low humidity (warm) furnace environment to more humid ambient conditions. Thus the term "delayed" is employed to distinguish from spalling immediately upon cooldown. This presumes of course that the much of the scale must be retained initially, most likely excluding scales formed on undoped, relatively high sulfur (>10 ppmw) alloys. Samples given some propensity for spallation would be most susceptible to M.I.D.S. Typically this means a range and combination of prerequisite factors: undoped alloys, intermediate, ~1-5 ppmw, levels of sulfur, high strain energy (> 5-10 μm thick), and cyclic damage exposing the scale-metal interface. This susceptibility is progressively decreased as sulfur is reduced below 1 ppmw, as Y, Hf, or Zr active element doping is employed, Pt additions made, or as high Al, e.g., Ni-50Al, compositions are used. For more adherent scales, a comparable degree of M.I.D.S. may take more cyclic damage, higher levels of humidity, higher levels of strain energy and longer time to be manifested.

Indeed a spectrum of M.I.D.S. behavior is seen as one or more of these factors are varied. It is helpful to view the phenomenon according to a spallation vs composition map that highlights "sweet spots" where M.I.D.S. may be most apparent, **Figure 3**. Using sulfur content as the major determinant of adhesion, a schematic representation can be constructed (taking cues from

adhesion maps for PWA 1480 [**4**]). Here, for moderate cyclic furnace oxidation exposures, a modicum of adhesion can be expected at ≤ 10 ppmw S and essentially full adhesion at ≤ 0.1 ppmw S, as approximated by the sigmoidal residual scale curve ***A*** after cooling:

$$\%Area_{ret'nd} = \frac{a}{e^{(b + c \log S)} + 1} \qquad (1)$$

where S is the sulfur content in ppmw,
a is between 0 and 1,
b and c are constants, generally between 0 and 4.

For *a=1*, *b=0,* and *c=2*, we obtain the symmetrical sigmoidal curve shown in **Figure 3a**, with an inflection point at 1 ppmw S and asymptotes at 0% retained scale for high S and 100% retained scale for low S. This locus can be shifted to the right (→), indicating higher adhesion at a given sulfur level, with reactive element dopants or Pt additions. Conversely, it can be shifted to less adhesion (←) if more strain energy is built up in the scale, i.e., with the scale thickness (oxidation time and temperature) and with the product, squared, of CTE mismatch times ΔT of cooling.

A second locus, curve ***B***, can be constructed (using *b=2*) to indicate the amount of retained scale following subsequent exposure to moisture. The amount of moisture-induced spallation is then represented as the cross-hatched region, shown in **Figure 3b** for ***Curve A - Curve B***, or "sweet zone" for M.I.D.S. Both ***A*** and ***B*** boundaries need to be considered to address the phenomenon: there may be too much initial spallation (before moisture exposure) to exhibit any additional spallation (band shifted left); or the adhesion may be so great and strain energy so low that no amount of moisture will trigger spallation (band shifted right). Curve ***B*** is also envisioned to shift to lower amounts of retained scale (←) and widen the sweet zone as the degree of additional moisture exposure, delay time, hydrogen charging, or amount of interfacial exposure (cyclic damage) increases. Residual interfacial stresses (tensile in the metal) may also be operative in attracting hydrogen into the interface and serve as an additive factor expanding this zone. Some specific examples will follow in the discussion of scale-metal interfacial failures, as in item III.C of the logic diagram outline, **Figure 1**.

Chemical basis

I.A H_2O reacts with Al powder to produce H_2 gas.

In the discussions of moisture-induced hydrogen embrittlement of Al, Ni_3Al, Fe_3Al and FeAl, it is often stated that water is chemically reduced by Al in the alloy to yield aluminum hydroxide (or aluminum oxide) and hydrogen according to eqn. 2:

$$Al_{alloy} + 3H_2O_{ambient} = Al(OH)_3 + 3H_{ads} \qquad [2a]$$

or:

$$2Al_{alloy} + 3H_2O_{ambient} = Al_2O_3 + 6H_{ads} \qquad [2b]$$

At this point, it is not critical to specify whether the oxide or hydroxide forms. It is specified that atomic hydrogen is produced, which directly allows for adsorption onto and absorption into the alloy. If the hydrogen solubility is exceeded locally or if recombination exceeds solution and

diffusion rates, H_2 gas may be evolved. Given the elusive nature of solved hydrogen and general difficulty of detection, H_2 gas evolution may offer an alternative means of verification by chemical analyses.

In that regard, we present the results of studies designed to evolve hydrogen gas by reacting Al powder in water [**Deng 5-7**]. Here, interestingly, the powder had to be modified to prevent instantaneous passivation and cessation of reaction. The authors pre-conditioned the powders by reacting (calcining) with substantial quantities of $Al(OH)_3$ at 600°C. The result is a γ-Al_2O_3 modified aluminum powder (GMAP), having apparent active sites on the metal preserved by contact with a stable, high diffusivity or porous oxide. Upon contact with liquid water, H_2 gas is evolved as measured by gas chromatography. For example, ~ 50 mole % of H_2 , relative to the amount of Al metal present, was recorded for reacting with water at 50°C for 7 hr, **Figure 3** [7].

These experiments with submerged Al powder represent an extreme compared to any reaction scheme between ambient moisture and an oxidized solid. For example, the degree of exposed metal is limited by the amount of scale cracking and spalling. The reaction should not occur for a completely intact healing scale. Secondly, the activity of Al in solution would be orders of magnitude than pure Al. Finally, observed spallation events occur in ambient humidity, much less than the saturated vapor pressure of liquid water. These differences would likely reduce the overall reaction, and the small amounts of reaction product may escape detection by most conventional techniques

Hydroxylation of alumina from adsorbed ambient moisture has also been discussed [**8** Al-Abadleh and Grassaian]. Here the pertinent reaction chemistry would be given by:

$$Al_2O_3 + 3H_2O_{ambient} = 2Al(OH)_3 \qquad [3]$$

But here it is apparent that hydrogen is not produced by reaction (3), and any detrimental effects on interfacial integrity would depend on the much slower diffusion of molecular water along the interface.

Other supporting evidence is provided by a study of copper reactions with water at room temperature [**9** H1]. Here 0.3mm thick copper sheet (140 cm^2) was exposed to low-oxygen content water in a closed vessel, with the vapor above the mix sealed by a palladium hydrogen permeability membrane. The other side of the membrane was high vacuum and connected to a mass spectrometer. It was found that H_2 gas was continuously generated over durations as long as 5000 hr. The explanation went as eqn. 2a, except that now the supposed metastable copper hydroxide reaction product was only enabled by the low oxygen content, with the adsorbed hydrogen of course combining and evolving as gaseous H_2.

I. Theoretical justification: Al_2O_3-H-metal bond

II.A. DFT ab initio calculations.

Given that exposed metal, containing reactive elements such as aluminum, will react with water and produce hydrogen as a by-product in some form, we then postulate that atomic hydrogen may enter the material by an adsorption/absorption sequence. Once at the interface, hydrogen may affect the strength of scale-metal adhesion. There is a growing body of work addressing the theoretical strength of alumina-metal interfaces and the effects of impurities and dopants,

through quantum chemical models and ab initio calculations. In general, sulfur has been found to significantly weaken the interface, in agreement with experimental findings [**10-13** Anderson, Bennett, Smith1,2] Reactive element dopants strengthen the interface while simultaneously binding sulfur and preventing mobility.

Interstitials, such as carbon and hydrogen, are not as widely studied, but the work of Smith et al. is relevant to the present case [**14-17**]. In that regard we cite his ab initio density field theory (DFT) study of C and H levels at the (0001) α-Al_2O_3 interface with 1/3 monolayers of (111) Co and Cu films. Here the lowest energy interstitial structure is determined over a range of C and H chemical potentials, producing the equivalent of a 2-D phase diagram for C and H surface atoms. It was found that 6 distinct structures resulted with specific C, H concentrations residing within a 2-oxygen atom surface cell. Next the work of adhesion for Co and Cu films is calculated for each stable configuration.

For purpose of illustration, the calculated values are displayed for each structure according to the alumina surface structure C-H composition in **Figure 5**. Actual data points corresponding to six stable structures are shown as the stars. (The 3-D mesh response surface is a conservative interpolation. It is displayed only for the purpose of illustrating overall trends, since the some grid points apply to unstable structures.) For the most part, it is seen that increasing H content results in a decrease in interface adhesion, for example, by as much as 90% in going from the 0H-3C structure to 3H-3C.

A similar trend is observed for Cu-Al_2O_3 interfaces, **Figure 6**, except that the overall magnitudes are about ½ those of Co-Al_2O_3. Furthermore, an analogous study by Smith et al, [**15**] calculates the work of separation to decrease from 7.02, to 4.72, to 0.63 J/m^2 for clean, 1/3 ML, and 1 ML, respectively, of interfacial hydrogen. Here 1 monolayer is defined as 1 H atom for every surface O atom.

Some limitations are acknowledged. There was no calculation for strictly hydrogen effects without carbon in figures 4 and 5; i.e., the clean interface value was determined only for the stable clean Al terminated α-Al_2O_3, while the C-H interface values were determined for O-terminated α-Al_2O_3 for the stable H-modified surface. For the specific case of alumina scales, the high Al activity corresponding to the low pO_2 of the interface results in an Al_2-terminated oxide. So the trends shown in **Figures 5 and 6** must be implicated for that more appropriate type of surface [**17** Jiang 2008].

II.B. Double Beam Interfacial T[illegible]ghness, Ni-X-Al_2O_3.

A negative effect of moisture on alumina-metal interface strength has been demonstrated by the fracture mechanics studies of Evans et al. and others. These generally entail diffusion bonded sandwiches of polished sapphire plates and ultra pure metals and alloys. Compression or bend bars are machined from the sandwiches, and exposed to a pre-drilled interface hole or pre-cracked by an overloaded Knoop microhardness indentation. The interface toughness is then resolved from the resulting crack growth behavior through classic K_{IC} relationships, as summarized in [**18** Evans1], reconstructed here as **Table I**.

In the first study [**19** Evans 2], the effect of ambient air was determined for the toughness of Ni-Al_2O_3 interfaces. First, in dry N_2 environments the interface toughness could only be estimated as >100 J/m^2 because the crack did not run along the interface. However it did follow the

interface and was reduced to 10 J/m^2 when measured in ambient (50% relative humidity) air. Carbon was a known interfacial impurity and behaved synergistically with moisture.

The toughness of Ni20Cr-Al_2O_3 interfaces was insensitive to ambient air because of the gettering effect of Cr and the stability of Cr-carbides [**20** Evans 3]. Again, the failure did not run along the interface so the toughness lower bound could only be estimated as >300 J/m^2. However when the composite was exposed to a 'liquid' phase anneal, above the melting point of any CrS precipitates, the interface failed in ambient air from residual thermal expansion mismatch stress, without the need for any external stress. Now the interface was contaminated with S and C. A toughness range of 2-7 J/m^2 could only be estimated. This data for Ni20Cr-Al_2O_3 emphasizes the negative synergy between moisture and sulfur. In a sense it fortells the "sweet zone" where moisture effects on scale spallation are maximized for interfaces that are partially compromised by some segregation and high strain energy.

A subsequent study examined the scale formed on a NiAl –coated superalloy [**21** Evans 4]. From scale buckling measurements vs applied compressive stresses, it was surmised that stable buckle delamination propagated with an interface toughness of only ~ 5 J/m^2 in moist air. The alloy contained no reactive element dopants, and therefore the segregation of impurities was presumed.

Finally the deformation of double cleavage drilled compression samples were evaluated in two environments at various sulfur segregation levels [**22** Bonnell]. It was found that increasing moisture (from oil to ambient humidity) at a given sulfur content decreased the interface toughness, as did further increases in the sulfur interface concentration.

The above experiments indicate the negative effect of moisture on bulk interfacial Ni- Al_2O_3 adhesion. Negative synergy between moisture, S, and C are indicated. However, it remains to be argued how hydrogen, according to the present mechanism, is created for less reactive Ni and NiCr alloys if there is no aluminum to react with moisture according to eqn. 2.

III. Interfacial Failures:

III.A. Bulk Aluminides.

A great deal of interest had been generated for potential high temperature, low density, oxidation resistant structural aluminides, specifically NiAl, Ni_3Al, FeAl and Fe_3Al. In the case of β-NiAl, room temperature ductility has still not progressed to conventional values, no matter what alloying schemes were adopted to maximize strength and no matter what testing conditions were adopted. In other words an intrinsically brittle material remained brittle. However in the case of the other aluminides, single crystals , microalloying, test conditions, and test environment had profound effects on room temperature ductility. The question of intrinsic and extrinsic grain boundary embrittlement became an issue, eventually reaching the atomic level of dislocation type and mobility. For a time, extrinsic embrittlement was simply precluded by ductility-enhancing B, Zr additions, until the true environmental effect was revealed. All the pertinent aspects of moisture induced embrittlement of aluminides have been expertly reviewed by key researchers, (Stoloff, Duquette, Liu, Chen) and form the basis of the summary below. [**23-26**].

The enigmatic behavior of so-called brittle intermetallics was finally resolved by early studies of FeAl and Fe_3Al that included a comparison of low tensile ductility measured under ambient conditions with higher values determined under vacuum or dry O_2. [**27,28** LML1,2]. The results

implicated ambient moisture (relative humidity) as the source of hydrogen, a notorious embrittling agent. It was already clear that cathodic hydrogen charging embrittled even the intrinsically ductile Ni_3Al+B,Zr alloys [**29,30** Kuruvilla Stoloff]. The broad spectrum of environmental effects can be seen by the telling nature of stress strain curves obtained under different conditions as shown in **Figure 7** [**23**]. Here the degree of plastic deformation in a tensile test can be seen to increase on a stress strain plot according to the decrease in hydrogen in the material or hydrogen or moisture in the test environment. The telling broad spectrum, ranging from 1% to 13% ductility, can be seen to vary from in situ continuous electrochemical hydrogen charging, pre-charging only, H_2 gas, moist air, dry air, to dry oxygen. Similar effects are presented for FeAl and Fe_3Al, **Figure 8**, where the overall embrittling trend follows vacuum, dry O_2, ambient air, 4%H_2/Ar, and H_2O vapor, with an anomalous effect for FeAl in vacuum [**27,28,33** Liu, McKamey, White].

Since hydrogen diffusion is involved, a time factor becomes apparent. In the case of tensile testing, strain rate dependence of embrittlement is often observed. Thus the above data was obtained at a constant strain rate of $3x10^{-6}$/s, generally low enough to allow any potential embrittlement to occur. Other data for Ni_3Al, obtained at or interpolated to 10^{-2}/s [**26** Chen], is shown in **Figure 9**. Here the ductility trend increases from 5%H_2/Ar , moist Ar, moist air, dry O_2, and vacuum [**31-33** George, Liu, Lee, White]. Another set of data varied the total pressure, but clearly related embrittlement to the effective p(H_2O), **Figure 10**. Here the ductility is seen to steadily decrease with p(H_2O) increasing from UHV (~10^{-9} Pa) to ambient conditions (~10^3 Pa). [**26,31,32** George, Liu, Pope; from Chen, Liu].

IV-A. Hydrogen Detected in Aluminides.

Chen and Liu [**26**] site a few studies indicating that hydrogen is produced by reaction of water with aluminides, e.g., ToF mass spectrometry showed a 4-20x increase in hydrogen for water treated Fe-36Al. Similarly, a temperature programmed desorption experiment with D_2O treated Ni_3(Al,Ti) revealed a D_2 peak at 350K, without any corresponding D_2O background peak. Here the implication is that the heavy water treatment did result in absorbed D_2 from reaction with the alloy.

V-A. Supporting Critical Experiments.

The demonstrations of embrittlement in H_2 –containing atmospheres or by cathodic hydrogen charging are strong evidence that the key factor in moisture induced embrittlement of aluminides is *hydrogen*. What can be taken from the studies of bulk aluminides is that any environmental source of moisture is a potential source of hydrogen and environmental (extrinsic) embrittlement. Thus various related phenomenon come to play depending on the specific test environment (strain rate, test temperature, adsorbed moisture, hydrogen dissociation, other grain boundary segregants), and the same framework can then be applied toward understanding M.I.D.S.

III.B. Anodic Films on Aluminum.

Another compelling analogy to moisture induced alumina scale spallation is presented by the thin films formed on aluminum and aluminum alloys. Moisture has been found to compromise thin native oxide films or those formed anodically or by electropolishing. Decohesion and loss of protection has been observed. In the extreme, hydrogen embrittlement of the alloy may result. Many of these features have been pointed out in the works of Scamans et al. and Shimizu, Skeldon, Thompson et al. [**34-38**]. The initial film is an amorphous alumina based on γ-Al_2O_3. Subsequent exposure to moisture involves the basic chemistry similar to that put forth for the

aluminide situation. Now boehmite (and pseudo-boehmite), AlOOH (· xH_2O) are observed in addition to $Al(OH)_3$ bayerite. But both reactions produce 3H atoms for every Al atom reacted, just as shown in reaction 2a,b above, enabling various hydrogen-induced phenomena [**35** S-R].

A telling experiment involved the exposure of electropolished Al and Al alloys to 100% relative humidity (saturated) air at 70°C. Bubbles, blistering, and scale-metal decohesion took place depending on the alloy and length of exposure, as long as condensed moisture was enabled. Nucleation of hydrogen bubbles at grain boundaries in sensitized alloys and dislocations was observed by TEM [**34, 35** Scamans; S-R]. An example of 5 μm bubbles formed in the film is shown in **Figure 11**. Here the native oxide was allowed to form by exposure to room air for 24 hr., followed by exposure to 70°C saturated air, inducing blisters of films on pure Al and Al alloys within minutes.

IV.B. H Detected under Alumina Films.

In general, the detection of hydrogen requires some specialized techniques. In the case of thin films on Al, moisture exposures have been characterized by glow discharge optical emission spectroscopy (GDOES). By depth profiling, hydrogen as well as various other aqueous impurities or alloy constituents may be identified in the film. For Al electropolished in CrO_3-H_3PO_4, GDOES has been used to obtain chemical profiles, showing H, Al, Cu, P, and Cr distributions. It is claimed that "...the surface film is hydrated across its thickness....the hydrogen profile exhibits two maxima at regions close to the surface and film/metal interface." [**36** Shimizu 1]. Othere studies characterized films produced by a wide variety of electrolytes [**37** Shimizu 2]. Here hydrogen distributions (and W, Mo, B, P, Si) were documented for films produced in sodium tungstate, ammonium pentaborate, sodium chromate, potassium permanganate, ammonium dihydrogen phosphate, and ammonium citrate electrolytes. In every case, a discernable H peak has been observed at the film-metal interface. Again this indicates a propensity for hydrogen released from the reaction of Al with moisture to segregate at the alumina-metal interface.

Nuclear reaction analyses (NRA), coupled with a high energy ^{15}N beam from an accelerator, was also used to characterize 200-250 nm anodic films grown on an Al-6.5 at.%W alloy in 0.1 M sodium tungstate [**38** Iglesias-Rubianes 3]. Distinct H enrichments were found at the film-alloy interface, in accord with the observations above. Enrichments on the order of 1.5 at.% H were proposed, as shown in **Figure 12**.

One final note added in proof is the GDOES profile of a *chromia* scale formed on SUS 430 stainless steel at 900°C after 6 hr. exposure to N_2-2.4%O_2-19.7%H_2O [**39** Yamuchi]. Here, again, a slight enrichment of hydrogen was detected at the vicinity of the scale-metal interface. Thus general support is given to the phenomenon of hydrogen segregation at scale metal interfaces in the presence of moisture.

V.B. Supporting Critical Experiments.

Strong support that hydrogen is the basis for moisture induced delamination of thin films is offered by the following study of externally applied hydrogen [**40** Liu,etal]. Here ion implantation of H^+ was performed on electropolished pure Al, anodized to produce films from 3-14 nm thick. After ion implantation with 100 keV H^+, at a fluence of $5x10^{13}$ ions/cm^{2}s and total dose of $6.6x10^{16}$ ions/cm^2, the films were noted to blister and peel off. It was further calculated that both implanted 10^{14} H^+ and 10^{15} aluminum vacancies were created in the near surface metal

area. Thus it could be theorized that either or both H^+ and Al vacancies may be responsible for film decohesion.

For this reason, the same laboratory engaged in subsequent experiments utilizing H^+, D^+, and $^3He^+$ ion implantation and comparable fluxes [**41** Bailey]. They found similar blistering and delamination for 60-110 keV H^+ and D^+ ions. An example of such delamination by H^+ implantation is shown in **Figure 13** for a 120 nm film. The circular features are indicative of individual blisters, while the large sheet is a continuous delamination of the film. Since the He^+ ions have up to 4x the mass of the hydrogen ions, they would be expected to produce many more vacancies. However no film deterioration was found for $^3He^+$ or $^4He^+$, even up to 270 keV. It was therefore concluded that the smaller hydrogen atom was the key to separation, not vacancy coalescence or He species. That is, the higher mobility of H compared to He near room temperature allows for accumulation of a hydrogen species at the oxide-metal interface. Furthermore, they identified a minimum dose of ~$3x10^{15}$ ions/cm^2, below which delamination does not occur, whereas extensive delamination did occur for $3x10^{16}$ ions/cm^2. Similarly, 60° off angle irradiation, resulting in only partial penetration of a 500 nm film, produced no damage, whereas 90° normal incidence, penetrating below the film, did result in blister formation.

III.C. Alumina Scales.

This finally brings us to the problem at hand, namely, moisture effects on alumina scale spallation. The experimental evidence for moisture induced delayed spallation spans two decades and many research groups. Recent reviews of our experience and various corroborating studies have summarized most instances of MIDS and the related desk top spallation (DTS) phenomenon for TBC's [JOM-TM, lesEmbiez]. The first dramatic exhibition, perhaps, occurred for scale stripping by water immersion of sulfur-purged NiCrAl [**43** Peterson]. Subsequently, the phenomenon has been documented for FeCrAl-X, PWA 1480, PWA 1484, Rene'142, Rene'N5, Rene'N6, plasma sprayed and PVD TBC's, LPPS NiCoCrAlY and Ni(Pt)Al aluminide bond coats, and no bond coat APS TBC systems [**3,44-61**].

Time delay. While the immersion test often produces immediate results, it is perhaps more problematic to document the natural delayed spallation process in ambient humidity. The latter is of practical significance since reproducibility problems may arise for typical cyclic oxidation testing due to uncontrolled test and measurement procedures. Addressing that issue, we present a time delayed spallation curve for a commercial Ni(Pt)Al coating on CMSX4, oxidized at 1150°C for up to 2000 1-hr cycles **Figure 14** [**3** Delayed]. It can be seen that continuous spallation, though slight, occurs well after cooldown, for perhaps as long as 24 hrs. It should be pointed out that this MIDS effect was correlated with surface rumpling at coating grain boundaries. Also, the overall behavior was still quite protective, exhibiting only a 3 mg/cm^2weight loss after 2000 cycles [**3**]. Less adherent scales would be expected to exhibit more rapid and extensive MIDS response, according to the schematic 'sweet zone' in **Figure 4** Conversely, more adherent systems would be expected to show less MIDS. This was demonstrated for a duplicate sample, with clearly reduced grain boundary rumpling, where essentially no MIDS was measured in exactly the same test as **Figure 14** [**3**].

Similarly, acoustic emission during immersion tests revealed extended time delays in spallation events. In this regard, samples of Rene'N5, with various Y levels, were oxidized at 1150°C for up to 1000 1-hr cycles. After cooldown, the samples were immersed in room temperature water

and monitored by acoustic emission [**52** Morscher]. The response of three samples, with nominal sulfur levels of 5 ppmw and Y levels of 88, 103, and 105 ppmw) is shown in **Figure 15a**. Note the intermittent rapid nature of the AE response, but spread over a period of ~24 hr. In contrast, hydrogen annealed samples revealed minimal activity, **Figure 15b.** The AE results for scale spallation were substantiated by the additional weight losses, number of spall segments, and spalled area due to immersion. Since these samples were Y-doped, desulfurization did not occur. The improved adhesion was possibly due to decarburization, from ~500 ppmw to 100 ppmw C. Any detrimental effect of carbon may be associated with a slight downward trend in ab initio predictions for work of adhesion, **Figure 5**.

Sulfur dependence. Desulfurization studies of PWA 1480 (by annealing in 5%H_2-Ar) provided a convenient process for removing sulfur in a controlled fashion [**64** JOM adhesions] according to the diffusion product, $4D_S t/x^2$, where D_S is the diffusion coefficient of sulfur at a given temperature, t is time, and x is sample thickness. Scale adhesion in 1100°C cyclic oxidation tests was mapped as a function of annealing condition, sample thickness and sulfur content. These results indicated that adhesion was maximized when the bulk sulfur content was reduced below that corresponding to an equivalent accumulation of 1 monolayer of segregated sulfur. For 0.5 mm samples, we arrive at a critical sulfur content of ~0.4 ppmw.

Above this value, moisture-induced spallation is observed; below it is insensitive. As an illustration of the sulfur dependence of MIDS, sample weights were recorded before and after exposure to moist breath or water immersion at 40, 200, and 500 cycles, **Figure 16**. It is seen that greater amounts of MIDS (up to 0.6 mg/cm^2) correlate with higher sulfur contents (5-7 ppmw S), and spallation decreases to almost the noise level below about 0.4 ppmw S. This is in accord with the schematic behavior shown in **Figure 3**, where the MIDS amount (= curve B-curve A), shrinks at lower sulfur contents. It is also noted that increased scale thickness and scale damage results in a corresponding MIDS increase in progressing from 40 to 200 hours of oxidation. This is equivalent to translating the envelope for MIDS, curve B, to lower sulfur contents because of higher stain energy and scale damage. However this trend reverses for the 500 hr data. Now, weight losses of 25 mg/cm^2 have been achieved for the high sulfur samples. Thus they have transitioned to less protective oxides, more spallation upon immediate cooldown, and less residual strain energy. This can be visualized as translating curve A to lower sulfur contents and convergence with curve B.

Thermal Barrier Coatings. Given the direct effect of alumina scale spallation on TBC life, moisture effects can be expected for TBC's relying on alumina-forming bond coats. Indeed such a phenomenon was first reported as blistering of an EB-PVD TBC over a pre-oxidized commercial Ni(Pt)Al bond coat under [Tolpygo and Clarke?]. Since the delamination was verified to be at the scale-metal interface by photoluminescence piezospectroscopy, it was surmised that moisture assisted slow crack growth was the operative process, analogous to moisture assisted slow crack growth in bulk alumina.

Moisture effects were monitored for plasma sprayed 250 μm 7YSZ TBC's tested in conventional cyclic oxidation [Smialek CESP11]. Here PWA 1484 substrates were used without a bond coat to exhibit a more direct effect of substrate sulfur content on scale adhesion and TBC life. Life was found to increase from 200 to 2000 cycles by decreasing the sulfur content from 1.2 to 0.01 ppmw. Furthermore, of the 8 surfaces coated, 6 failed by delayed desk top spallation (DTS). On

the 0.01 ppmw S sample, one failed upon cool down, (CD) and one surface did not fail until immersed in water (H_2O).

Similar tests were performed for commercially applied EB-PVD YSZ coatings, with a Pt-aluminide bond coat, on Rene'N5 substrates [**57** SZC 13]. Thermal cycling inevitably resulted in DTS for all 6 coatings tested at both 1135°C with 45 minute cycles and at 1150°C with 60 minute cycles. Failure occurred only after removal from the test apparatus and exposure to true ambient conditions, room temperature and relative humidity. In some cases the coatings could be made to fail simply by the application of a water drop. A video recording has been made of another sample that remained intact after cool down, but then failed completely within 10 seconds of applying two water droplets [**57**]. The phenomenon has been verified by Rudolphi, Renusch, and Schütze for an LPPS NiCoCrAlY bond coat followed by an EB-PVD YSZ TBC, preoxidized at 1050°C for 310 hr [**58**]. Their results also show acoustic emission triggered by the water drop application and complete failure within 5 seconds. This is in contrast with the absence of AE or spallation for as-coated samples treated identically.

As a demonstration of this phenomenon, we report on a recent video of a TBC failure for a 1st stage, high pressure turbine blade, pulled from actual engine service. Approximately 1 cm high chord sections were machined from the blade and these were further sectioned into ~ 1 cm wide samples. The cleaned samples were placed in a alumina boat, oxidized at 1200°C, and weighed at intervals of 1, 5, 10, 15, and 20 hr. Some sections failed upon coodown. If a section did remain intact, a water drop was applied by means of a wash bottle. At least one section failed at each examination time after 1 hr. A sequence of still frames captured from one failure video is shown in **Figure 17** for a 15 hr exposure. The first frame shows the application of the water stream, i.e., 0.0 seconds. (The superimposed time code is in units of [hr:min:sec:1/30 sec.]) After 21 seconds of moisture exposure, coating delamination initiates at the upper right corner (arrow). A corresponding chip has spalled off in the next 0.3 sec. In the next 0.2 sec., adjacent sections delaminate explosively and are caught in mid-flight along with some water droplets (arrows). Most of the spallation is complete in another 0.2 seconds, with the stable resting appearance obtained in the final ½ second frame. This 1 second total sequence documents the dramatic nature of moisture-induced TBC failure. It underscores the potential critical nature of moisture effects for coatings and scales reaching high levels of stored strain energy. There is little possibility of true slow crack growth according to classic chemical hydroxylation of alumina. It appears that the interface had been sufficiently weakened during the 21 second immersion and was ready to fail upon any crack initiation.

Many TBC DTS characteristics are unambiguously elucidated and confirmed in the recent thorough study of Deneux et al. [**61** Monceau, OxMet in press]. Here duplicate samples of conventional EB-PVD TBC samples, using a Ni(Pt)Al bond coat on 0.5 ppmw sulfur AM1 superalloy, were exposed in cyclic furnace tests at 1150°C (45 min. hot duration, 15 min. forced air cooling to 80°C). Successive exposures, ranging from 75 to 360 cycles, established a threshold water drop delamination life of ~ 170 cycles, considered as the most dependable or "real" lifetime. However, coatings survived 200 cycles of normal cycling when maintained in the furnace environment. When the latter samples were exposed to ambient humidity at room temperature, the coatings failed by DTS in a few minutes (or within 38 seconds after applying a water drop). Furthermore, coatings stored in dry air at room temperature survived, metastably, for 48 hr., as they too failed within a few minutes after subsequent exposure to ambient

humidity. Microstructural examination also revealed cracks in the γ'-$(Ni,Pt)_3Al$ coating surface, which can be considered as further evidence in support of the proposed hydrogen embrittlement mechanism.

Their study underscores a potential uncertainty or drawback to current TBC FCT protocol. If the samples are allowed to remain at furnace test conditions, they may give misleading spallation lives. Alternatively, intrinsic scatter will be built into this life test depending on any variance of exposures to ambient conditions (such as remote inspection or sample weighing) and the relative humidity of the locality or laboratory environment. It has been argued that relative humidity can be increased by about a factor of 40x in removing a sample from a 100°C environment and cooling to ambient conditions, because of the high saturation moisture level at 100°C compared to that at 21°C [delayed spallation].

IV.C. H Detection under Alumina Scales.

Support for MIDS by hydrogen detection under a mature alumina scale due to moisture exposure is difficult task. First, detection through a thick scale is problematic, especially considering interface roughening due to sputter profiling for spectroscopy. Secondly, detection directly after exposure of an interface to moisture is a problem for high vacuum systems. Given these issues, alternative or modified techniques may be required. In that regard, an effort was undertaken to detect hydrogen under an alumina scale formed on a VPS NiCoCrAlY, with an APS YSZ top coat. Oxidation was performed at 1100°C for 75-1200 hr. [**56** Zschau et al; **60** Rudolphi et al. DECHEMA]. Hydrogen was analyzed by a specialized proton induced gamma emission [P.I.G.E.] technique. Basically, 5 keV N ions are used to bombard the sample and identify H by the emission of gamma rays according to the nuclear reaction $^{1}H(^{15}N, \alpha\gamma)^{12}C$. Samples were exposed in dry or 2.5, 10 and 50v/o H_2O moist air. The interface was exposed by a 4-pt. bend fracture, in a vacuum pre-chamber to avoid any contamination before transfer and analyses in to the P.I.G.E. chamber. Generally a hydrogen signal corresponding to 0.1-2 at. % was detected a few hundred nm into the metal, but with no distinguishable interfacial concentrations, other than a system generated peak. Furthermore, at this time no large differences between as-received, dry and wet oxidation samples was obtained, **Figure 18**. There may be a basic difference in hydrogenation behavior between the isothermal oxidation in moist air (studied here) and cyclic oxidation followed by exposure to ambient humidity (generally required to give rise to MIDS and DTS phenomena).

V.C. Supporting Critical Experiments.

Electrolytic cathodic charging is a technique often used to demonstrate hydrogen embrittlement. Since hydrogen had been proposed as the key factor responsible for MIDS and DTS according to reaction [2] above [**2**], cathodic charging was then attempted to support the hypothesis. Thus, well characterized samples of Rene'N5+Y, pre-oxidized at 1150°C for 1000 1-hr cycles, immersed in water to leave only highly adherent scales [Morscher; and Pint], were later subjected to hydrogen charging in 1N H_2SO_4, a commonly employed electrolyte. In order to minimize gaseous H_2 evolution, the current vs voltage response was carefully mapped in 0.1 V increments. It was found that at ~ -2.0V, a measurable current was first observed, amounting to ~ 0.5 mA. (This is a relatively benign condition compared to the typical 100 mA currents employed for cathodic charging of bulk material). Samples charged at this -2.0V knee in current response were examined intermittently and weighed for hold times of ~10 min. up to 1 hr., both before and after applying the voltage. Results shown in **Figure 19** illustrate that no additional spallation occurred for simple immersion, without any applied potential. However, measurable weight loss resulted from cathodic charging, decaying with time, as all the scale was removed

and with no particular correlation of loss rate with current. Optical macrographs revealed successive areas of spallation with time, as shown by the start/finish insets, confirming that the weight loss was due to scale removal. Subsequent SEM studies identified the characteristic alumina grain imprints in the exposed metal interface [2]. One note added in proof is the catastrophic swelling and cracking of the alloy that occurred when a bare Rene'N5+Y sample was subjected to overcharging at -3.0V and ~100mA, **Figure 20**. Here it can be seen that the alloy was severely blistered and cracked at many levels, even etched down to the scale of individual γ'particles. Indeed, some degree of hydrogen embrittlement has been reported for fatigue tests of the superalloy PWA1480 resulting from high pressure hydrogen charging [**63,64** Gayda, Gayda]. As a further note added in proof, reverse (anodic) polarization, at the respective +1.3 V knee, resulted in slow, but continuous weight loss due to alloy dissolution, producing a closely correlated weight loss rate – current dependence. All in all, this set of experiments was consistent with interfacial scale delamination due to hydrogen charging. Accordingly they support the aspect of MIDS and DTS presuming hydrogen as the key factor in moisture effects.

High temperature H_2O causes H to be incorporated into M-Al alloys.
As evidence that hydrogen can enter alloys and reach critical levels, we cite the work of Subanovic et al. in which a plasma sprayed sample of NiCoCrAlY was oxidized in an Ar-4%H_2-2%H_2O gas [**65** Subanovic]. Here oxidation at 1100°C for 72 hr allowed H to penetrate the scale along Y-rich Yttrium Aluminium Perovskite (YAP) YAlO3 oxide stringers and reach the metal. This continuous process eventually resulted in swelling and blistering of the sample from H_2 gas pressure, **Figure 21**. It was found that both H_2 and H_2O components were required to produce swelling, indicating that the moisture reaction with Al (eqn. 1) was again involved. In this case, the reaction was at high temperature where hydrogen solubilities and diffusion are substantially increased. So instead of just local damage at the scale metal interface, the hydrogen is able to reach much higher levels in the bulk volume of the metal.

It is recalled that a SUS 430L stainless steel, oxidized at 900°C for 6 hours in N_2-2.4%O_2-19.7%H_2O, incorporated hydrogen in both the scale and alloy [**39** Yamauchi 2004]. It was detected by thermal desorption mass spectroscopy by reheating samples up to 750°C in vacuum. The maximum amount of dissolved hydrogen in the scale was estimated to be ~0.3 mole %. In addition, the use of glow discharge optical emission spectroscopy revealed a small, but measurable, hydrogen enrichment in the vicinity of the oxide scale –metal interface.

Discussion

From the reactivity of activated aluminum powder (GMAP) with liquid water, generating H_2 gas, we can expect some measure of reaction between adsorbed moisture and Ni-Al alloys, with the potential of a hydrogen by-product. This would affect oxidized samples only if the scale-metal interface is exposed by partial spalling or thru-cracks in the scale. Thus fully intact scales are less prone to the moisture effect.

The ab initio studies provide a predictive trend for Co-Al_2O_3 interfacial weakening by H interstitials. Further reductions in the work of adhesion appear possible with interfacial carbon. This is consistent with numerous measures of MIDS on Rene'N5+Y, where moisture effects were more pronounced for material oxidized in the as-received condition. By comparison, hydrogen annealed samples, which reduced the carbon content, exhibited remarkable MIDS

resistance. Also, interfacial toughness measurements of bulk Al_2O_3-Ni samples indicate weakening to both moisture (in ambient air) and sulfur segregation.

The embrittlement of aluminides in ambient (humid) atmospheres provided the original impetus for the present line of thinking [**1,2** JOM]. The chemical reactivity of bulk intermetallic alloys to that of Ni_3Al phases in bond coats and superalloys is likely to be similar enough to result in the same type of hydrogen formation and adsorption. The embrittlement of Ni_3Al compounds or PWA 1480 and Rene'N5+Y γ/γ' alloy in hydrogen containing gas or by cathodic hydrogen charging, respectively, suggests that scale interfaces may be sensitive to other sources of hydrogen besides moisture. Indeed, cathodic charging has caused massive interfacial de-scaling of otherwise perfectly adherent scales formed on hydrogen annealed Rene'N5+Y. It may also be surmised that MIDS and DTS may be avoided in vacuum or dry O_2, as was indeed shown for TBC's [**61** Deneux]. It has yet to be demonstrated whether H_2-containing gases will lead to MIDS, although they have produced H_2-induced gas bloating of a conditioned NiCoCrAlY alloy [Subanovic]. Finally, since B and other dopants mitigated the environmental embrittlement of Ni and Fe aluminides, it might be also expected to have beneficial effect regarding MIDS and DTS for thermally grown alumina scales.

The sensitivity of thin amorphous alumina films (on aluminum alloys) to moisture provides an extremely close analogy to the case of thermally grown alumina scales (on Ni-Al high temperature alloys and coatings). The observation of moisture induced blisters, de-scaling by H-implantation (not He), and detection of interfacial H under the amorphous films strongly implicate hydrogen as the key to the weakened interface. This then applies to MIDS for thermally grown scales as well, and one might expect hydrogen injection by suitably conditioning pre-oxidized samples in hot water and detection by GDOES [**66** Hayashi].

Thus, many of the conditions for exhibiting MIDS and DTS have been addressed and cross referenced to hydrogen based phenomena. A source of hydrogen is a pre-condition (as in ambient moisture and adsorption at lower temperatures at high relative humidity). The scale must have some damage, as from extensive thermal cycling, to allow access to an exposed metal interface. The interface should possess a high residual (biaxial tension) stress level, such as would result from a thick scale with high strain energy, after cooling from high temperature. Progressive spallation would be time dependent, allowing for some element of hydrogen diffusion ahead of the damaged area. These effects are most evident in a hypothetical "sweet zone," where the sulfur content is low enough (or reactive elements high enough) to maintain the scale upon initial cooling, but not so low as to preclude spallation altogether. In that regard, cathodic hydrogen charging was still found to remove the most adherent of scales on hydrogen annealed Rene'N5+Y.

Summary

This monograph has attempted to highlight relevant moisture-induced weakening phenomena from a number of related fields and relate them to the scale spallation issue. Following the logic tree presented in **Figure 1**, we have started with the basic reactivity of liquid water with activated aluminum metal, showing that hydrogen gas is yielded as a by-product. Detrimental humidity effects were predicted by ab initio oxide-metal calculations and born out experimentally in fracture mechanics studies of alumina-Ni bi-samples. Ambient humidity has embrittled aluminides and other intermetallics, again producing H as a by-product of reactive aluminum and water. Time-sensitive properties were consistent with hydrogen diffusion as a pre-requisite for embrittlement. Grain boundary interfacial failure was a common attribute, and hydrogen was detected in the bulk alloy. Thin native, electropolished, or anodic films on aluminum alloys were sensitive to blistering by exposure to room temperature moisture. The treated films revealed a hydrogen concentration at the film-metal interface by various techniques. Hydrogen, but not He, implantation was also capable of delaminating these films.

Many studies of moisture induced scale spallation and desk top spallation of TBC's now exist. Various researchers have investigated systems exhibiting the "sweet zone" of a scale or TBC system with relatively good adhesion, but having some cyclic damage and the high strain energy of mature scale. The key condition is to retain the scale upon normal cooldown or in the low humidity of the furnace environment, then produce a time delayed failure by unintentional or deliberate exposure to high humidity. Dedicated, sophisticated efforts are underway to identify hydrogen under the scale as a result of these moisture reactions. But, nevertheless, auxiliary exposures, by cathodic hydrogen charging or exposure of a special microstructure to an Ar-H_2-H_2O mixed gas, have produced remarkable results, e.g., complete de-scaling or catastrophic blistering of the alloy, respectively. Both are completely consistent with hydrogen-driven phenomena. In all, the logic tree approach has structured many findings that, at present, appear in concert with the proposed mechanism that hydrogen embrittlement is the root cause of moisture-induced failure of protective alumina scales.

References

1. J.L. Smialek, "Moisture Induced Spallation and Interfacial Hydrogen Embrittlement of Al_2O_3 Scales," NASA Technical Memorandum, 2005-214030, December, 2005.
2. J.L. Smialek, *JOM*, **1**, 29-36 (Jan., 2006).
3. J.L. Smialek, Moisture Induced Delayed Spallation of Alumina Scales on a Ni(Pt)Al Coating, NASA TM 2009-215664, June (2009); also Oxidation of Metals, in press.
4. J.L. Smialek: "Maintaining Adhesion of Protective Al_2O_3 Scales," *JOM*, January 2000, pp. 22-26.
5. Z.Y. Deng, Y.F. Liu, Y. Tanaka, J. Ye, and Y. Sakka, Modification of Al Particle Surfaces by γ-Al_2O_3 and Its Effect on the Corrosion Behavior of Al, J. Amer. Ceram. Soc., 88 (2005) 977-979.
6. Z.Y. Deng, Y.F. Liu, Y. Tanaka, H.W. Zhang, J. Ye, and Y. Kagawa, Temperature Effect on Hydrogen Generation by the Reaction γ-Al_2O_3- Modified Al Powder with Distilled Water, J. Amer. Ceram. Soc., 88 (2005) 2975-29779.
7. Z.Y. Deng, J. Ferreira, Y. Tanaka, and J. Ye, Physiochemical Mechanism for the Continuous Reaction of γ-Al_2O_3- Modified Aluminum Powder with Water, J. Amer. Ceram. Soc., 90 (2007) 1521-1526.
8. H.A. Al-Abadleh and V.H. Grassain, FT-IR Study of Water Adsorption on Aluminum Oxide Surfaces, Langmuir, 19 (2003) 341-347.
9. G. Hultquist, et al., Catal. Lett., DOI 10.1007/s10562-009-0113-x, published online 28 July 2009.
10. S.Y. Hong, A.B. Anderson, J.L. Smialek, Surface Science, 230 (1990), 174-183.
11. W. Zhang, J.R. Smith, X-G. Wang, and A.G. Evans, Phys. Rev. B 67 (2003) 245414.
12. I.J. Bennett, J.M. Kranenburg, and W.J. Sloof, J. Am. Ceram. Soc. 88 (2005) 2209-2216.
13. J.R. Smith, Y. Jiang, and A.G. Evans, Int. J. Mat. Res. 98 (2007), 1214-1221.
14. W. Zhang, J.R. Smith, and A.G. Evans, Acta Mat., 50, (2002), 3803-3816.
15. X-G Wang, J.R. Smith, and M. Scheffler, J. Am. Cerm. Soc., (2003) 696-700.
16. X.G. Wang and J.R. Smith, Physical Review B, 70 (2004) 081401
17. Y. Jiang, J.R. Smith, and A.G. Evans, Applied Physics Letters, 92 (2008) 141918
18. A. G. Evans, J.W. Hutchinson, and Y. Wei, Acta mater., 47 (1999) 4093-4113.
19. F. Gaudette, S.Suresh, A.G.Evans, G. Dehm, and M. Ruhle, Acta mater. 45 (1997) 3503-3513.
20. F.G. Gaudette, S. Suresh, and A.G. Evans, Metall. Mat. Trans., 31A (1999), 1977-1983.
21. J.S. Wang and A.G. Evans, Acta mater. 46 (1998) 4993-5005.
22. D.A. Bonnell and J. Kiely, phys. stat. sol., 166 (1998) 7-17.
23. N.S. Stoloff and D.J. Duquette, *JOM*, **45**, (1993)30-35.
24. C.T. Liu, "Ni_3Al Aluminide Alloys," in *Structural Intermetallics*, R.Darolia, et al., eds., TMS, Warrendale, PA, 365-377, (1993).
25. N.S. Stoloff, "Hydrogen and Moisture-Induced Embrittlement of Nickel and Iron Aluminides, in *Hydrogen Effects in Materials*, A.W. Thompson, N.R. Moody, eds., TMS,

Warrendale, PA, 523-537 (1996).

26. G.L. Chen and C.T. Liu, International Materials Reviews, 46 (2001) 253-270.
27. C.T. Liu, E.H. Lee, and C.G. McKamey, "An Environmental Effect as the Major Cause for Room Temperature Embrittlement in FeAl," *Scripta Metall.*, **23**, 875-880 (1989).
28. C.T. Liu, C.G. McKamey, and E.H. Lee, Scripta met., 24 (1990) 385-390.
29. A.K. Kuruvilla and N.S. Stoloff, Scripta met. (1985) 83-88.
30. A.K. Kuruvilla and N.S. Stoloff, "Hydrogen Embrittlement of Ordered Alloys," in Mat. Res. Soc. Symp. Proc. 39 (1985) 229-238.
31. E.P. George, C.T. Liu, D. Pope, Scripta metall. mat., 30 (1994) 37.
32. E.P. George, C.T. Liu, and D.P. Pope, Scripta metall. mat., 44 (1996) 1757.
33. K.H. Lee and C.L. White, Scripta metall. mat., 33 (1995) 129.
34. G.M. Scamans, J. Mat. Sci., 13 (1978) 27-36.
35. G.M. Scamans and A.S. Rehal, J. Mat. Sci., 14 (1979) 2459-2470.
36. K. Shimizu, H. Habazaki, P. Skeldon, G.E. Thompson, and G.C. Wood, Surf. Interface Anal. 27 (1999) 998-2002.
37. K. Shimizu, G.M. Brown, H. Habazaki, K. Kobayashi, P. Skeldon, G.E. Thompson, and G.C. Wood, Electrochemica. Acta. 44 (1999) 2297-2306.
38. L. Iglesias-Rubianes, P. Skeldon, G.E. Thompson, U. Kressig, D. Grambole, H. Habazaki and K. Shimizu, Thin Solid Films. 424 (2003) 201-207.
39. A.Yamauchi, Y. Yamauti, Y. Hirohata, T. Hino, and K. Kurokawa, TDS Measurement of Hydrogen Released from Cr_2O_3 Scale Formed in N_2-O_2-H_2O Atmospheres, Electrochemical Society Proceedings, E. Opila, T. Maruyama, T. Narita, E. Wuchina, J. Fergus, J. Mizusaki, and D. Schifler, eds., The Electrochemical Society, Pennington, NJ, (2004) 93-100.
40. Y. Liu, M. Alexander, E. Koroleva, P. Skeldon, G.E. Thompson, P. Bailey, T.C.Q. Noakes, K. Shimizu, and H,. Habazaki, Surf. Interface Anal. 33 (2002) 318-321.
41. P.Bailey, T.C.Q.Noakes, Y. Liu, M.R. Alexander, E.V. Koroleva, P. Skeldon, G.E. Thompson, H. Habazaki, K. Shimizu, Nuclear Instr. Meth. in Phys. Res. B. 197 (2002) 265-270.
42. J.L. Smialek, Materials Science Forum, Vols. 595-598 (2008) pp 191-198. (Also NASA TM 2008-215206. June 2008, 9 pages).
43. J. L. Smialek: "Adherent Al_2O_3 Scales Formed on Undoped NiCrAl Alloys," N. L. Peterson Mem. Symp. Proc. on Oxidation and Associated Mass Transport, TMS-AIME Oct. 6-9, 1986, pp. 297-313.
44. D. R. Sigler, Adherence Behavior of Oxide Grown in Air and Synthetic Exhaust Gas on Fe-Cr-Al Alloys Containing Strong Sulfide-Forming Elements: Ca, Mg, Y, Ce, La, Ti, Zr," *Oxidation of Metals*, **40**, 555-583 (1993).
45. M.A. Smith, W.E. Frazier, and B.A. Pregger, *Mat. Sci. Engineer.*, **A203**, 388-398 (1995).
46. V. Sergo and D.R. Clarke, *J. Amer. Ceram. Soc.*, **81** [12] 142-161 (1998).
47. J.L. Smialek: "Toward Optimum Scale and TBC Adhesion on Single Crystal Superalloys,"

High Temperature Corrosion and Materials Chemistry, E.J. Opila, P.Y. Hou, D.Shores, M. McNallan, and R. Oltra, eds., The Electrochemical Society Proceedings, volume 98-9, Pennington, NJ, 1998, pp. 211-220.

48. R. Janakiraman, G.H. Meier, and F.S. Pettit, *Metall. and Mat. Trans.*, 30A, (1999) 2905-2913.
49. V. Tolpygo, D.R. Clarke, *Mater. Sci. Eng.*, **A278**, 142-161 (2000).
50. J. L. Smialek and B. A. Pint, *Mater. Sci. Forum*, **369-372**, 459-66 (2001). (also NASA TM 2000-210362).
51. J.L. Smialek, *Ceramic Engineering and Science Proceedings*, **23**, 4, 485-495 (2002).
52. J.L. Smialek and G.N. Morscher, *Mater. Sci. Engineer. A*, **332** (1-2), 11-24, 2002.
53. M.C. Maris-Sida, G.H. Meier, and F.S. Pettit, "Some Water Vapor Effects during the Oxidation of Alloys that are α-Al_2O_3 Formers," *Metall. Trans.*, **34A**, (2003) 2609-2619.
54. D. Renusch, H. Echsler, M. Schütze: Mat. High Temp., 21 (2004), 65-76.
55. K. Onal Hance, "Effects of Water Vapor on the Oxidation Behavior of Alumina and Chromia Superalloys between 700°C and 1000°C, Ph.D. Thesis, University of Pittsburgh (2005).
56. H. Zschau, M. Dietrich, D. Renusch, M. Schütze, J. Meijer, H. Becker, *Nucl. Instr. Met.B*, **249**, 381-383 (2005).
57. J.L. Smialek, Dongming Zhu, and Michael D. Cuy, Scripta mat., **59** (2008) 67-70; also NASA TM 2008-215210, (April, 2008).
58. M. Rudolphi, D. Renusch, M. Schütze, , *Scripta mat.*, 59 (2008) 255-257.
59. M. Rudolphi, D. Renusch, H.-E. Zschau, and M. Schütze, Materials Science Forum, Vols. 595-598 (2008) 177-184.
60. M. Rudolphi, D. Renusch, M. Schutze, and J. Meijer, ICMC-TF, 2009-D-09-00171.
61. V. Deneux, Y. Cadoret, S. Hervier, and D. Monceau, Oxid. Met., (2009), in press.
62. J.L. Smialek, *JOM*, January 2000, 22-26.
63. J. Gayda, R.L. Dreshfield, T.P. Gabb, "The Effect of Porosity and γ/γ' Eutectic Content on the Fatigue Behavior of Hydrogen Charged PWA 1480," *Scripta Met. et Mat.*, **25**, 2589-2594 (1991).
64. J. Gayda, T.P. Gabb, and R.L. Dreshfield, "The Effect of Hydrogen on the Low Cycle Fatigue Behavior of a Single Crystal Superalloy," in *Hydrogen Effects on Material Behavior*, N.R. Moody, A.W. Thompson, eds., TMS, Warrendale, PA, 591-601 (1990).
65. S. Subanovic, D. Naumenko, M. Kamruddin, G. Meier, L. Singheiser, and W.J. Quadakkers, Corr. Sci., 51 (2009) 446-450.
66. J.L. Smialek and S. Hayashi, unpublished research.

Table 1. Effect of moisture on Ni(Cr)-Al_2O_3 interfacial fracture toughness (from [19-22]).

Figure Captions.

1. Conceptual outline showing top-down logic structure for the proposed hydrogen effect in moisture induced delayed spallation of alumina scales.
2. Schematic of moisture-induced hydrogen embrittlement used to explain delayed spallation of alumina scales and desk top TBC spallation: A marginal Al_2O_3 – metal interface, under high stress, is exposed to a moist environment; local electrochemical cells produce $(OH)^-$ to react with Al_{metal}, leaving H^+ to diffuse into the interface. With time, H diffusion progresses underneath the scale, further weakening the scale and allowing spallation to occur.
3. Figure 2. Schematic of scale retention after cooling and subsequent exposure to moisture. a) Total spallation occurs at high sulfur contents, transitioning to total adhesion at low sulfur contents. Curve A corresponds to surface after cooling, Curve B corresponds to surface after moisture induced spallation. b) The amount of observable moisture induced spallation (Curve A – Curve B) is maximized as a "sweet zone" having intermediate adhesion.
4. Water-induced H_2 evolution from reaction with (γ-Al_2O_3 - modified) Al powder, showing ~ 50% completion after 7 hr at 50°C. (after Deng, et al., [5].)
5. Ab-initio prediction of hydrogen-induced Co-Al_2O_3 interfacial weakening (symbols for 2-D stable arrangements). Interpolation/extrapolation surface of DFT calculations of Smith et al., [16]
6. Ab-initio prediction of hydrogen-induced Cu-Al_2O_3 interfacial weakening (symbols for 2-D stable arrangements). Interpolation/extrapolation surface of DFT calculations of Smith et al., [16].
7. The embrittlement effects of hydrogen and moisture in tensile stress/strain behavior of Fe_3Al; strain rate = $3x10^{-6}$ /s. (from Stoloff and Duquette, [23]).
8. Reduced tensile ductility of FeAl and Fe_3Al due to moisture and H_2 (after Liu, McKamey, White in [27,38,33]).
9. Reduced tensile ductility of Ni_3Al due to moisture and H_2; strain rate = $1x10^{-2}$ /s. (after George, Liu, Pope, Lee, White [31-33]).
10. Reduced tensile ductility of Ni_3Al due to $P(H_2O)$ estimated from total pressure. (in Chen and Liu [26], taken from George, Liu, Pope [31-32]).
11. Moisture induced blisters in native alumina film on aluminum from exposure to water vapor saturated at 70°C. (from Scamans and Rehal, [35]).
12. Preferential hydrogen segregation at anodic oxide - aluminum metal interfaces by nuclear reaction analyses. Pre-anodized in 0.1 M Na_2WO_4 at 20°C. (from Iglesias-Rubianes, et al. [38]).

13. H-implantation induced bubbles and blister failure of an anodic alumina film on aluminum. FEG-SEM micrograph of 120 nm film, 110 keV D^+ ions, $1x10^{17}$ions/cm^2 (from Bailey et al., [41]).

14. Delayed alumina scale spallation after cycling Ni(Pt)Al - coated CMSX4 at 1150°C. Weight change and time after initial measurement in ambient air. 1- hr cycles. (from Smialek [3]).

15a. Delayed spallation detected by acoustic emission during water immersion. Rene'N5+Y oxidized at 1150°C for 1000 1-hr cycles. (from Smialek and Morscher [52].

15b. Minimal delayed spallation during water immersion for Rene'N5+Y, hydrogen annealed at 1250°C for 100 hr prior to oxidation at 1150°C for 1000 1-hr cycles. (from Smialek and Morscher [52].

---

16. Effect of sulfur content on the amount of moisture induced spallation after cyclic oxidation of PWA1480 at 1100°C. 1-hr cycles. (from Smialek [42]).

17. Water-induced spallation of an EB-PVD TBC on a commercial DS superalloy HPT blade pulled from service and oxidized at 1200°C for 15 hr. Approximately 1 cm x 1cm trailing edge section; 20 second incubation, 1 second spallation times.

18. P.I.G.E. hydrogen concentration profiles in a NiCoCrAlY bond coat before and after oxidation in 1100°C air at various moisture contents. TBC removed by in situ 4-pt. bend. Initial peak is interpreted as a chamber artifact. (from Rudolphi, Renusch, Schutze, and Meijer [60]).

19. Cathodic hydrogen charging and descaling of Rene'N5+Y. Hydrogen annealed at 1250°C for 100 hr prior to oxidation at 1150°C for 1000 1-hr cycles. No spallation after 1 hr immersion in 1N H_2SO_4 with no applied volatage. Complete stripping in 20 minutes at -2.0V, 0.5-1.0 mA charging. (after Smialek [2]).

20. Massive blistering, cracking, and etching of unoxidized Rene'N5+Y subjected to cathodic hydrogen overcharging at -3.0 V, ~100 mA (from Smialek [2]).

21. Catastrophic internal voidage and swelling for free-standing plasma sprayed sample of NiCoCrAlY oxidized in an Ar-4%H_2-2%H_2O gas at 1100°C for 72 hr. (from Subanovic et al. **[65]**). Oxidation in Ar-20%O_2 produced no such unusual effect.

---

a) Optical macrophotos of exposed surface; b) SEM micrographs of cross sections

---

Ambient Air Effect on Interfacial Toughness

Table 1. Effect of moisture on Ni(Cr)-Al_2O_3 interfacial fracture toughness (from [19-22]).

metal	oxide	atmosphere	segregant	J/m^2 toughness	
Ni	Al_2O_3	dry N_2	C	>100	Gaudette, Suresh, Evans, Dehm, Ruhle [19]
Ni	Al_2O_3	air*	C	10	
Ni20Cr	Al_2O_3	air*, dry N_2	C, no S	>100-300	Gaudette, Suresh, Evans [20]
Ni20Cr	Al_2O_3	air*	C, S**	2-7	
NiAl	Al_2O_3***	air*	yes	5	Wang, Evans [21]
			****		
Ni	Al_2O_3	oil	0.19	34.2	Bonnell, Kiely [22]
Ni	Al_2O_3	air	0.19	19	
Ni	Al_2O_3	air	0.45	17.7	
Ni	Al_2O_3	air	0.55	8.5	

* 50%RH@20°C

** ~3%@ surface

***TGO, 1-100 hr @ 1000°, 1100°C

****S/Ni AES ratio

Table I

Moisture-Induced Delayed Spallation of Alumina Scales

The Hydrogen Factor

Logic Tree

I. Chemical Basis:

$2Al_{alloy} + 3H_2O_{ambient} = 2Al(OH)_3 + 3H$

II. Theoretical justification:
Al_2O_3 -H-metal bonding

III. Interfacial failures:

A. Aluminides **B.** Anodic films **C.** Thermal Scales

H detected

Supporting critical experiments

F1

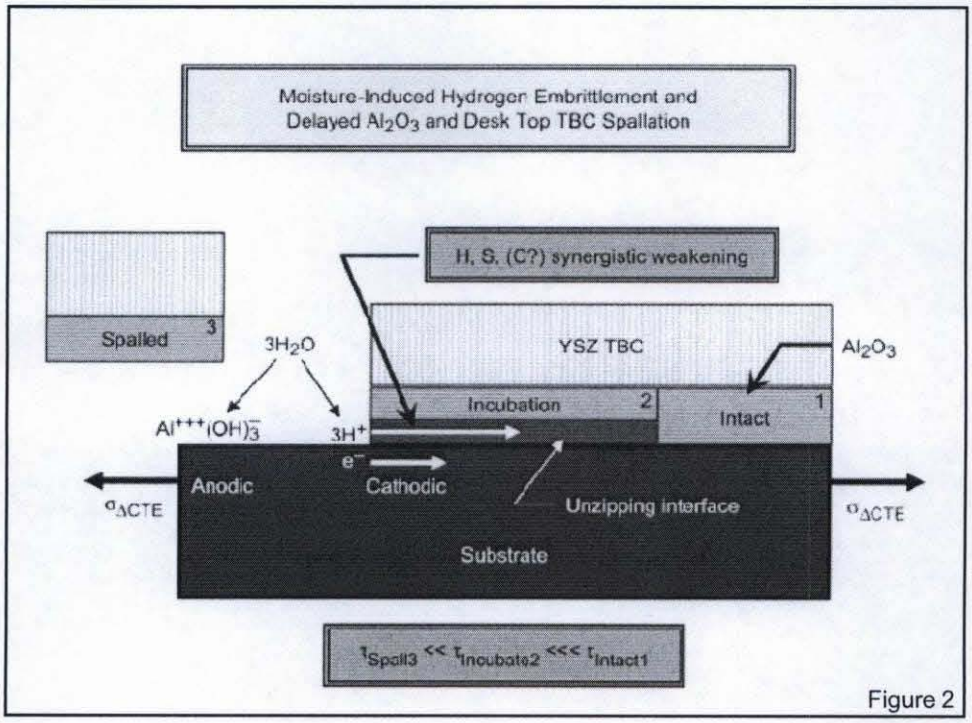

Figure 2

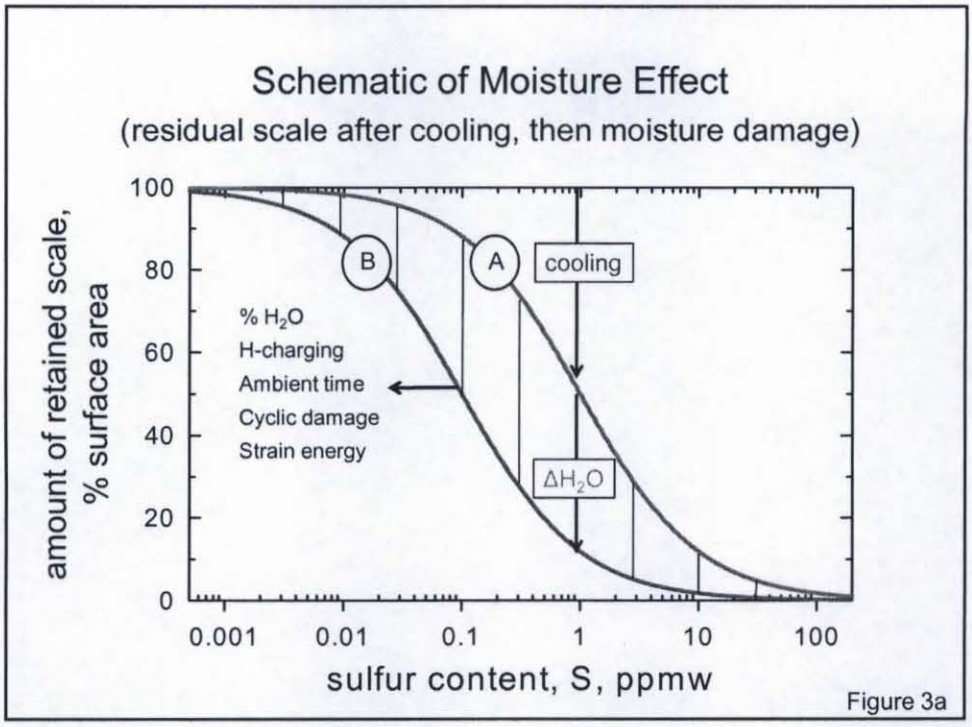

Figure 3a

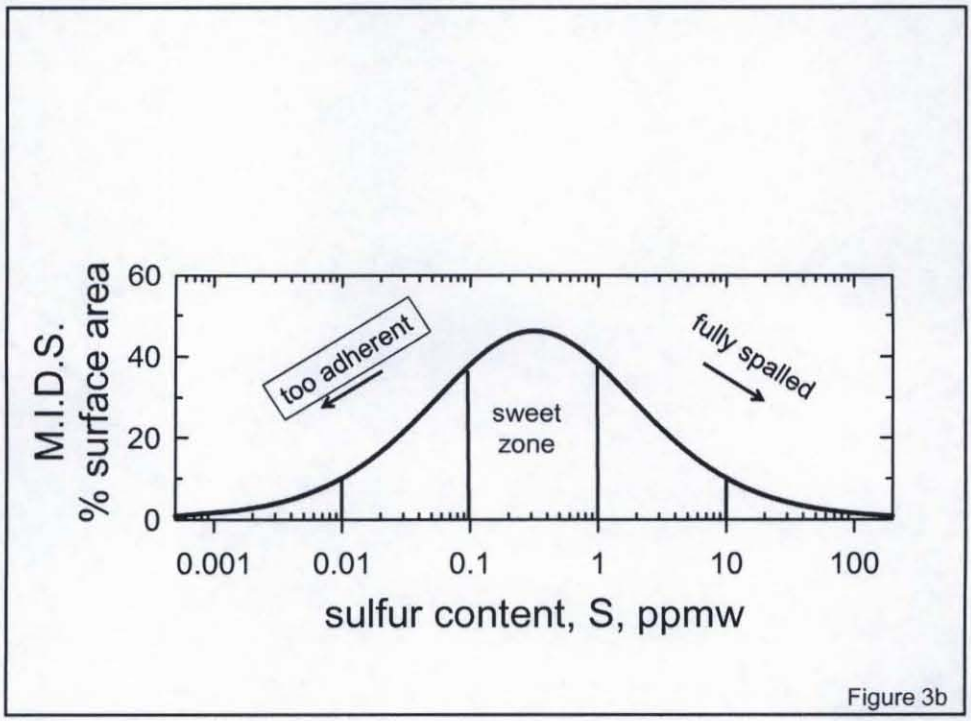

Figure 3b

I. Hydrogen Produced by H_2O–Al Reaction

(after Deng, Liu, Tanaka, Zhang, Ye, Kagawa

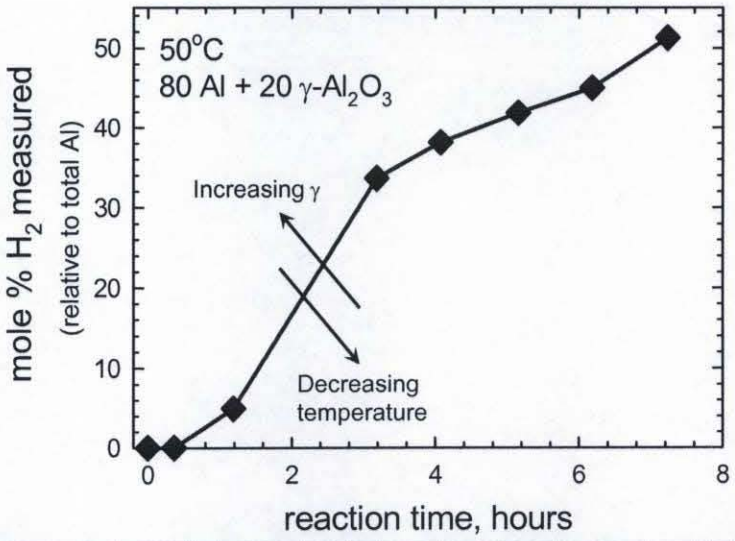

Figure 4

Ab-Initio Models Predict H Reductions of Co-Al_2O_3 Interfacial Strength

C,H per 2-oxygen atom surface cell
(after X.G. Wang, J.R. Smith, Phys Rev B, 2004)

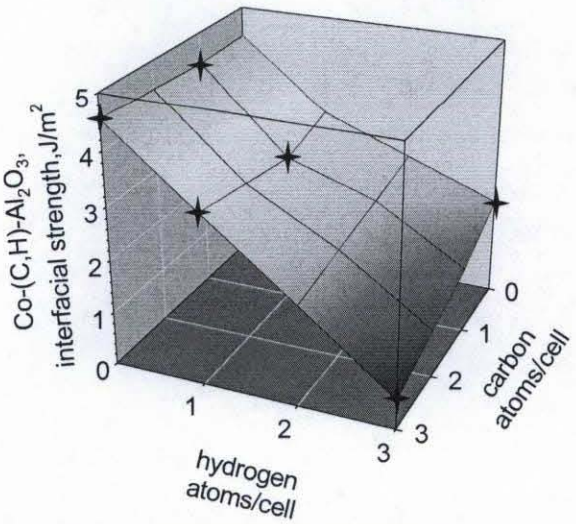

Figure 5

Ab-Initio Predictions
C,H Effects on Cu-Al_2O_3 Interfacial Strength

C,H per 2-oxygen atom surface cell
(Wang and Smith, Phys Rev B, 2004)

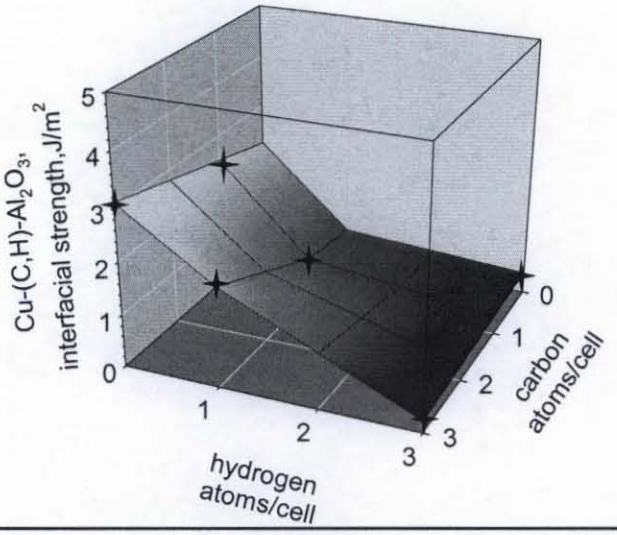

Figure 6

Effect of Hydrogen and Moisture
on the Tensile Ductility of Ni_3Al
(after Scott in Stoloff and Duquette)

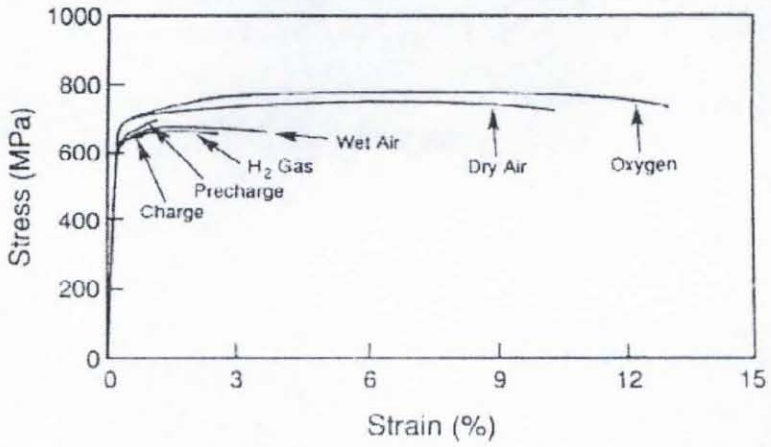

Figure 7

Moisture and Hydrogen Effects on Fe_3Al and FeAl Ductility

(after Liu, McKamey, and Lee)

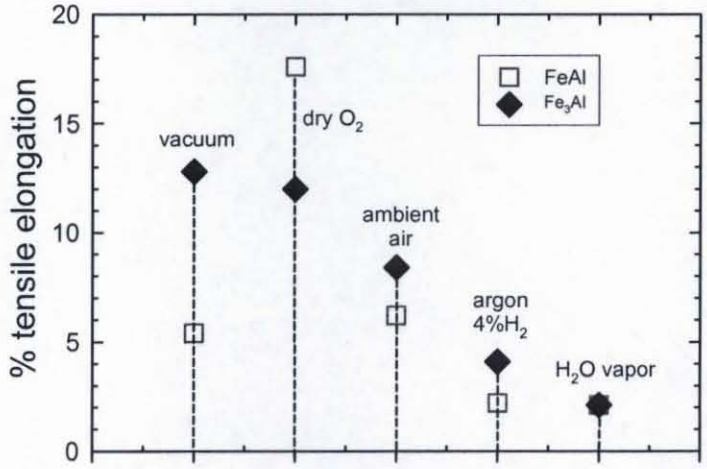

Figure 8

Moisture and Hydrogen Effects on Ni_3Al Ductility

(after Lee and White)

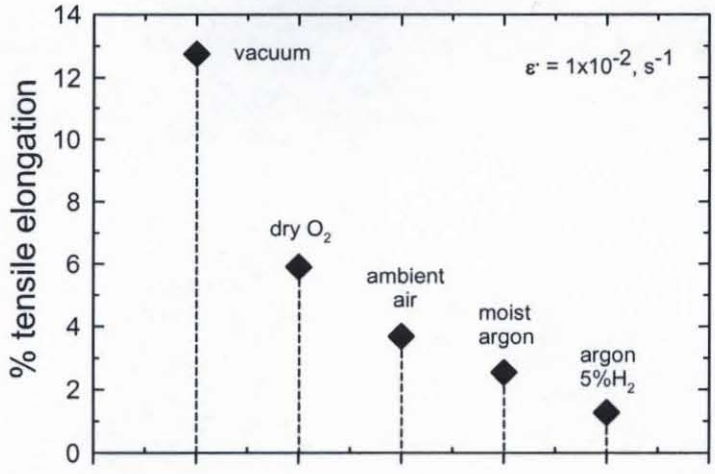

Figure 9

Moisture Effects on Ni_3Al Ductility

(after George and Liu, et al)

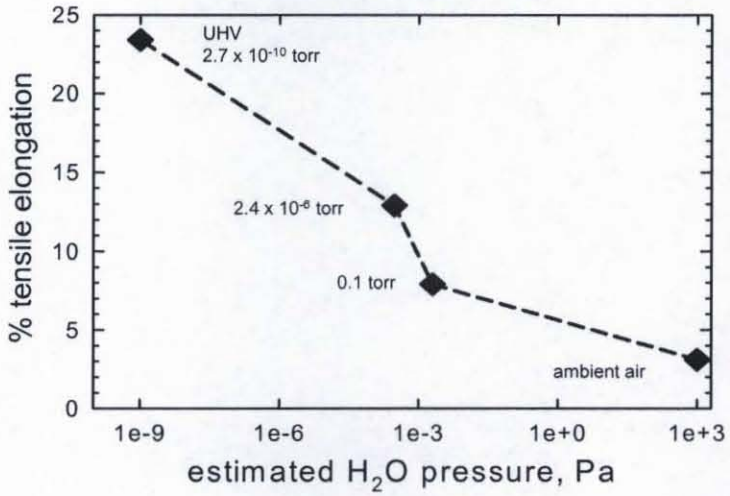

Figure 10

Moisture Induced Blisters on Al

(G. M. Scamans and A.S. Rehal)

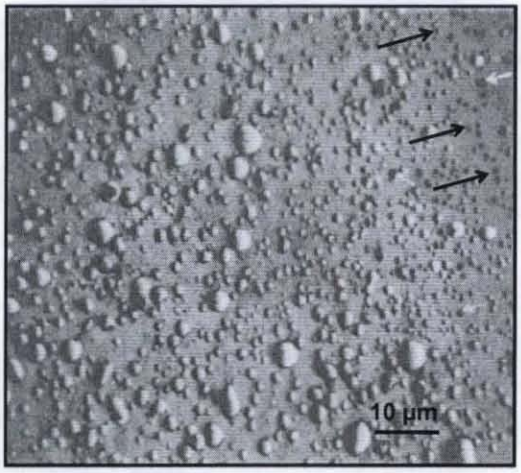

Surface film blisters on superpurity aluminium after reaction with water vapor saturated at ~70° C. Note the hemispherical nature of the blisters and the dark circular islands of reaction after blister fracture (arrowed).

Figure 11

Hydrogen Segregation at Anodic Film/Al Interfaces

(L. Iglesias-Rubianes , P. Skeldon, G.E. Thompson,
U. Kreissig, D. Grambole, H. Habazaki, K. Shimizu)

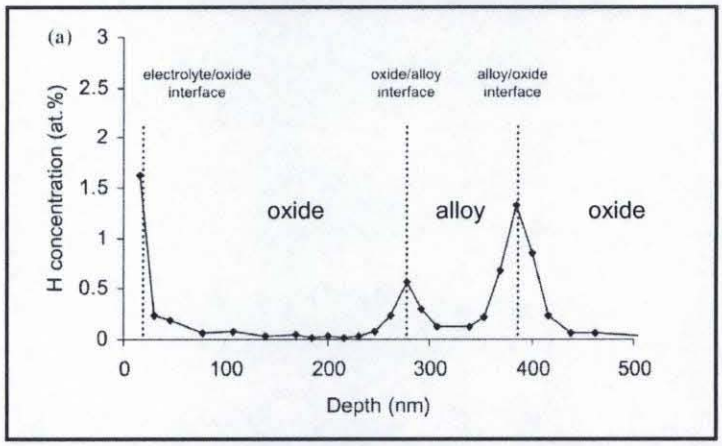

Distribution of hydrogen, determined by NRA, for Al–6.5 at.% W alloy
(Anodized in 0.1 M sodium tungstate electrolyte at 293 K)

Figure 12

Hydrogen Bubbles and Blistered Anodic Film on Al

(P.Bailey, T.C.Q.Noakes, Y. Liu, M.R. Alexander, E.V. Koroleva,
P. Skeldon, G.E. Thompson, H. Habazaki, K. Shimizu)

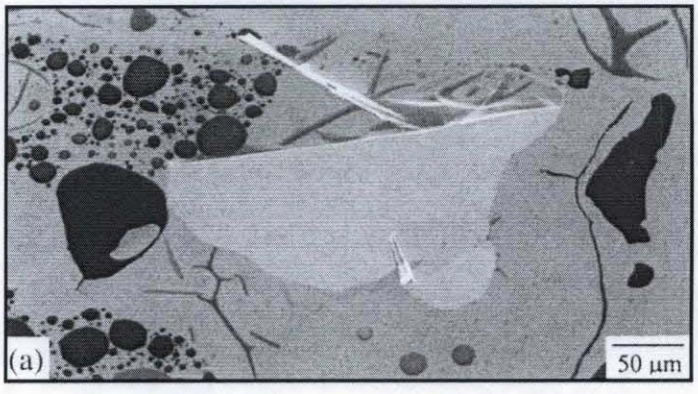

FEG-SEM micrographs of the surface of the oxide of 120 nm thickness irradiated with 110 keV D^+ ions at 90° incidence with a fluence of (a) 1 x 10^{17} ions cm^2

Figure 13

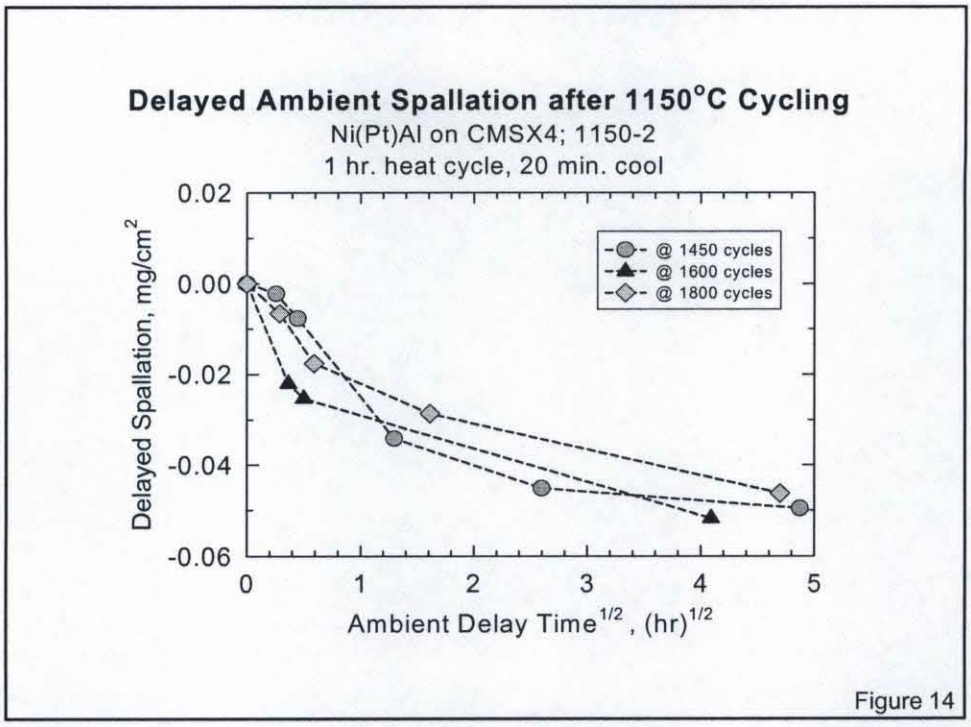

Figure 14

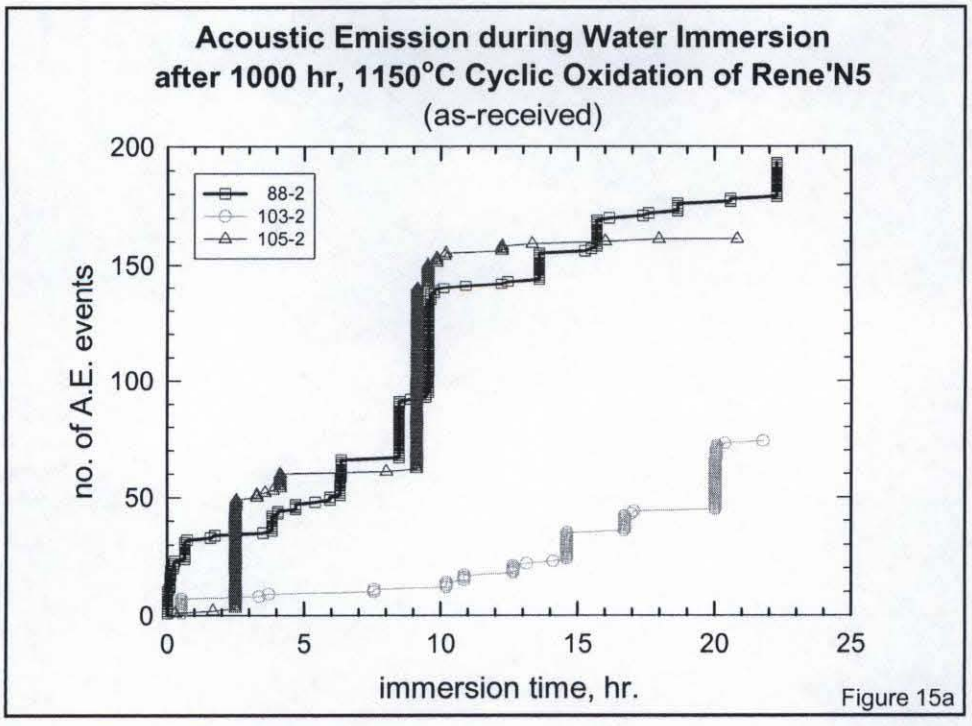

Figure 15a

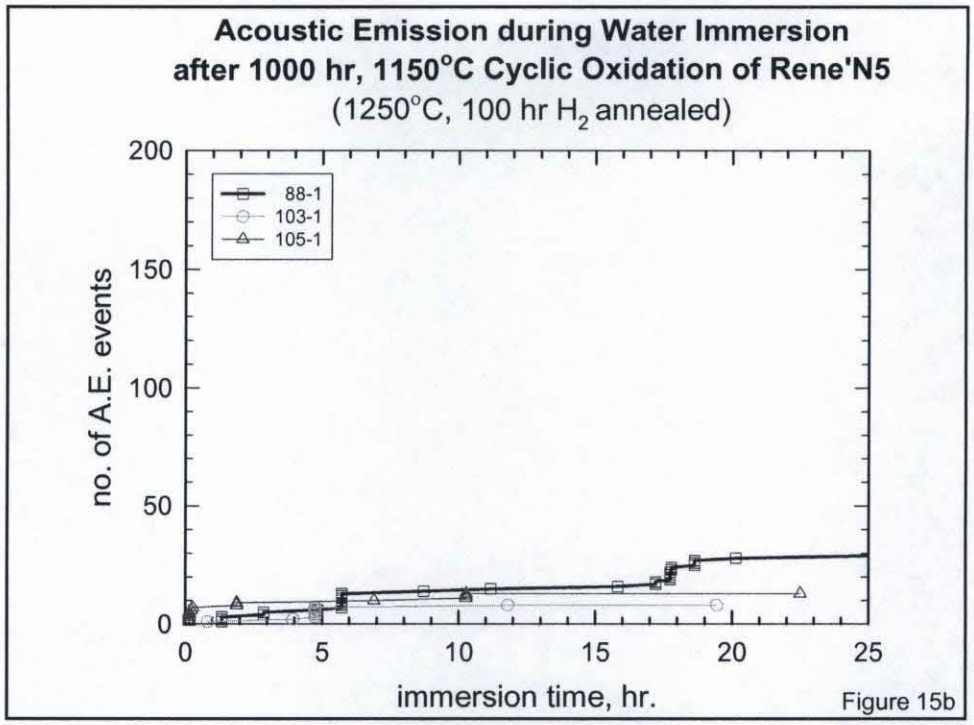

Figure 15b

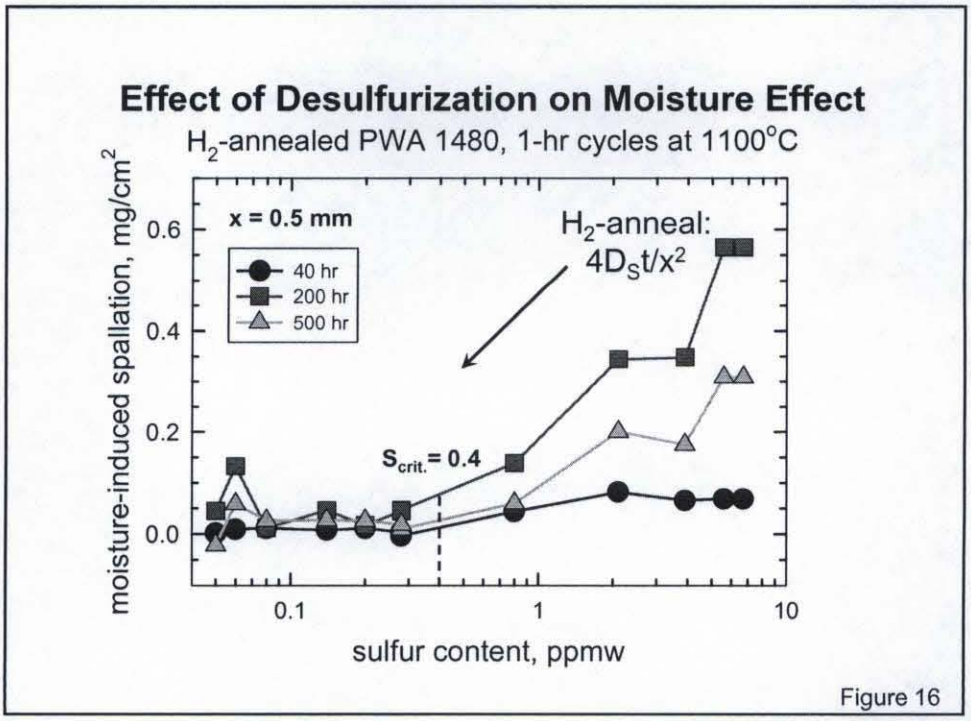

Figure 16

Water Drop Failure Sequence of a TBC, 1st Stage HPT Blade Section

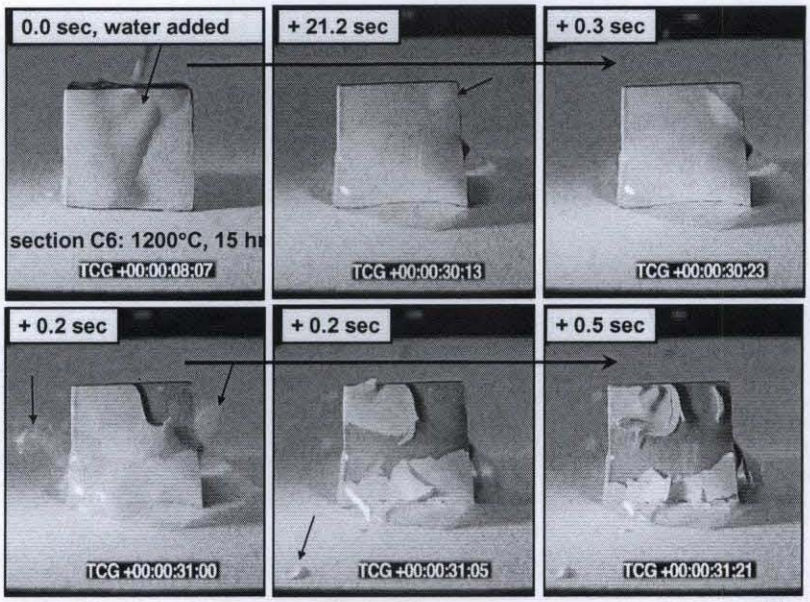

Figure 17

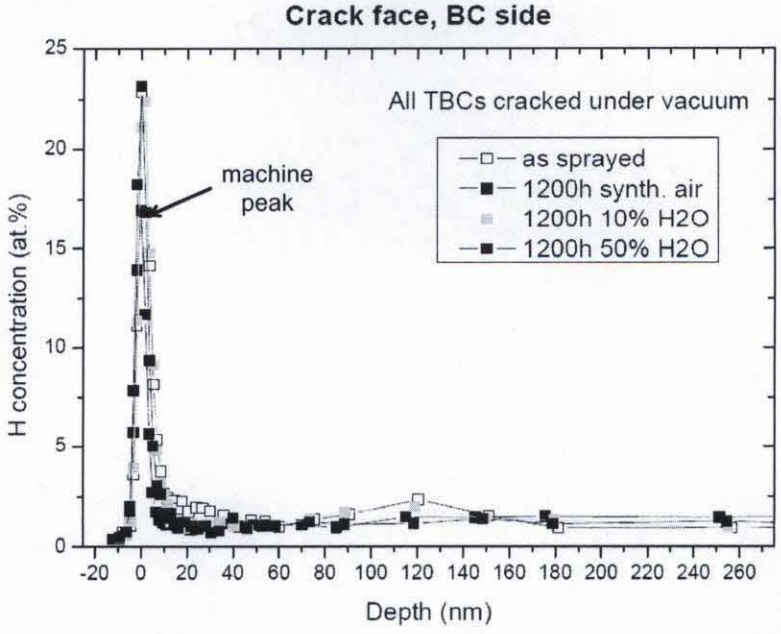

Figure 18

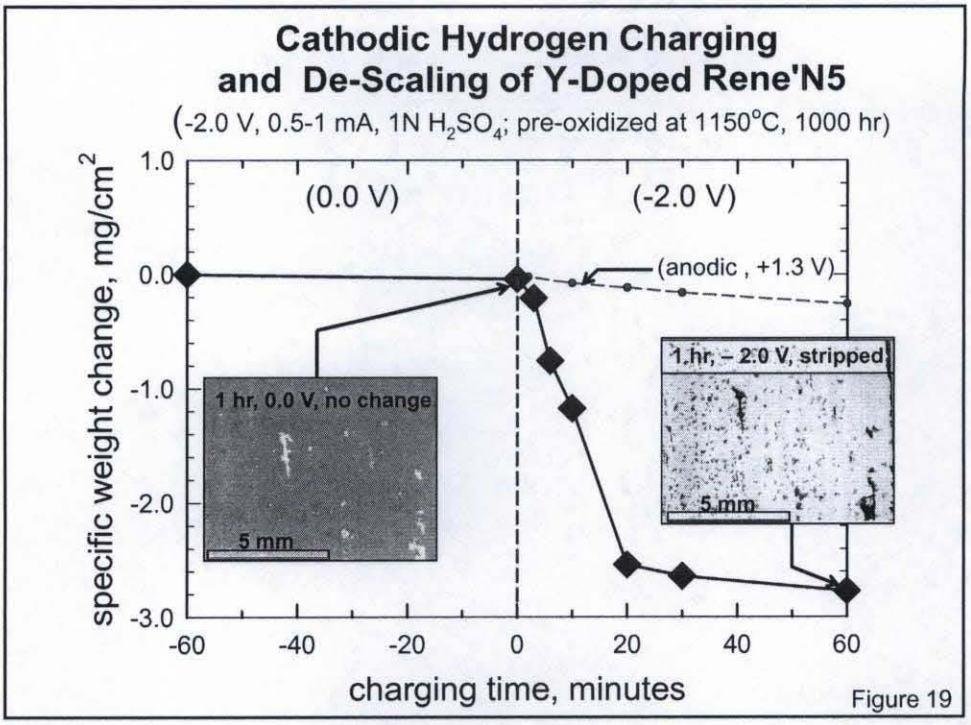

Figure 19

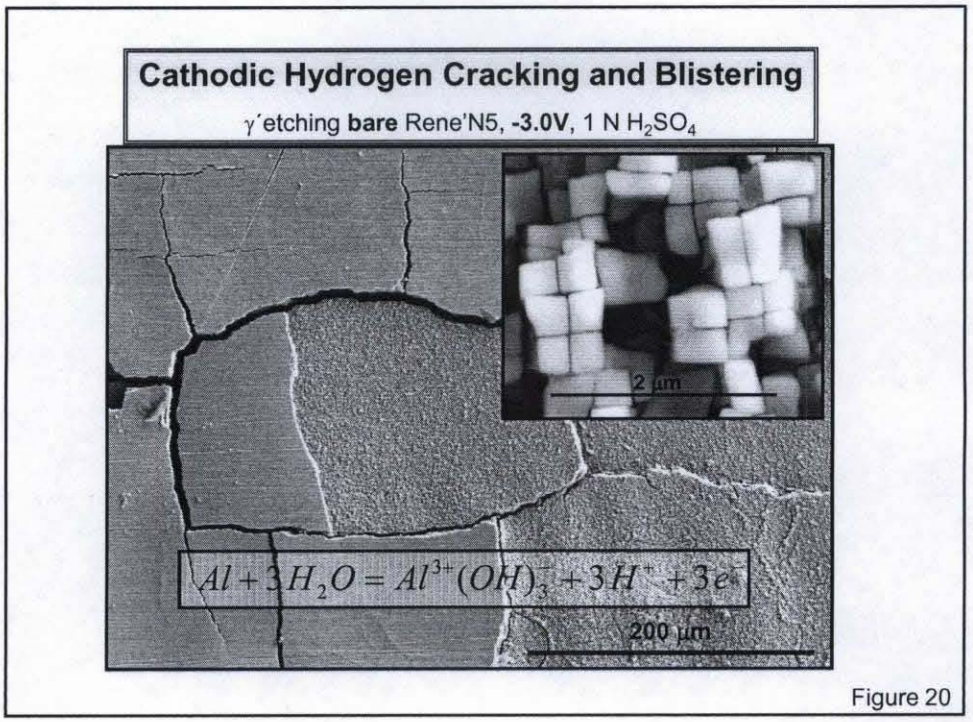

Figure 20

Hydrogen-Induced Blistering of NiCoCrAlY

M. Subanovic, D. Naumenko, M. Kamruddin,
G. Meier, L. Singheiser , W.J. Quadakkers

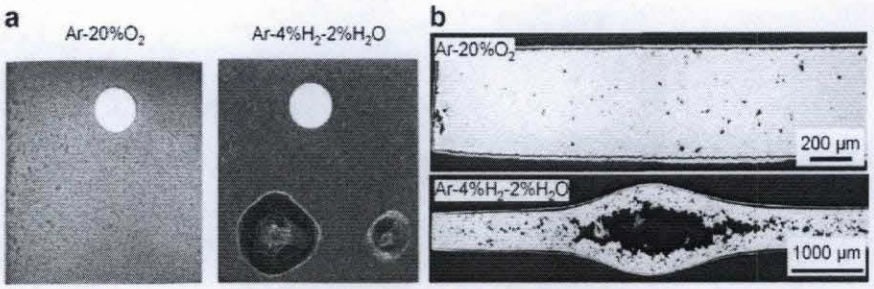

Optical (a) macro and (b) metallographic cross-sections of free-standing NiCoCrAlY-coating after exposure at 1100°C for 72 h in test gases indicated.

Figure 21